Vol. **106** (2004) *ACTA PHYSICA POLONICA A* No. 2

Proceedings of the XXXIII International School of Semiconducting Compounds, Jaszowiec 2004

Elastic Properties of Zinc Blende MnTe

P. Djemia*, Y. Roussigné, A. Stashkevich

Laboratoire des Propriétés Mécaniques et Thermodynamiques des Matériaux
UPR CNRS 9001, Université Paris Nord
Av. J.B. Clément, 93430 Villetaneuse, France

W. Szuszkiewicz, N. Gonzalez Szwacki, E. Dynowska,
E. Janik, B.J. Kowalski, G. Karczewski, P. Bogusławski

Institute of Physics, Polish Academy of Sciences
al. Lotników 32/46, 02-668 Warsaw, Poland

M. Jouanne and J.F. Morhange

Laboratoire des Milieux Désordonnés et Hétérogènes
Université Pierre et Marie Curie
B.P. 86, 75015 Paris Cedex 05, France

The Brillouin light scattering was used to investigate elastic properties of the zinc blende, MBE-grown MnTe layer that was deposited on a (001) GaAs substrate covered by CdTe buffer layer. The three elastic constants of the zinc blende MnTe, namely c_{11}, c_{12}, and c_{44}, were directly determined for the first time from the frequency of the Rayleigh mode, of the pseudo-surface mode, and of the shear horizontal bulk mode traveling parallel to the layer surface. The value of c_{11} was checked using the frequency of longitudinal bulk waves propagating at different angles from the normal of the layer plane. This value was also independently determined by results of the folding of acoustic phonons, observed for MnTe/CdTe superlattices by the Raman scattering. Finally, the bulk modulus given by the formula $B = (c_{11}+2c_{12})/3$ was determined for zinc blende MnTe by *ab initio* calculations making use of the density functional theory and atomic pseudopotentials; spin polarization of MnTe was taken into account. A satisfactory agreement between theoretical and experimental values was obtained.

PACS numbers: 62.20.Dc, 75.50.Pp, 78.35.+c

*corresponding author; e-mail: djemia@galilee.univ-paris13.fr

1. Introduction

The determination of the mechanical properties, specifically elastic properties of thin layers deposited on a substrate is important for both physical models and engineering application purposes. Indeed, a lot is known about the elastic properties of bulk materials, but in most cases, information concerning thin layers is scarce and sometimes unreliable. This is mainly due to the difficulties in measuring such properties with appropriate and accurate tools, although the deposition and the structural characterization techniques have significantly progressed during the last few years, providing better materials with an improved knowledge of their microstructure. Nowadays, there are only few widely used techniques for such mechanical measurements, namely, the surface Brillouin light scattering (BLS) [1], the picosecond ultrasonics [2], the Bulge/Blister test [3], the vibrating reed device [4], the nano-indentation [5], combined X-ray with *in situ* tensile test [6] and micro-tensile tests [7, 8]. Most of the time, one needs to use a combination of these techniques in order to fully determine their elastic constants or moduli. In the case of low-dimensional structures the elastic constants are of particular importance, because they describe the strain resulting from the lattice mismatch as well as the influence of this strain on various physical properties of the system under investigation.

Zinc blende (ZB) MnTe is a well-known magnetic semiconductor, which has been an object of intensive studies for the last fifteen years. Its lattice parameter value $a_0 = 6.338$ Å [9] is not far from values of several II–VI type semiconducting compounds (it matches rather well with them) so such MnTe is often applied as a constituent of II–VI quantum structures, also these used in spintronic experiments. However, bulk ZB MnTe crystals do not exist in nature because of the metastable character of this phase (the stable modification of this compound is hexagonal MnTe, crystallizing in NiAs-type structure) (for details see, e.g., [10]). Due to this, values of the elastic constants for ZB MnTe cannot be determined directly by the standard ultrasound measurements and are not well known. Present, limited knowledge on these values is given by the extrapolation of the mechanical properties of the mixed crystal $Cd_{1-x}Mn_xTe$ (measured in the composition range $x \leq 0.52$) [11]. The analysis of the results of the high-resolution, X-ray diffraction (HRXRD) spectra taken for CdTe/MnTe and ZnTe/MnTe superlattices ([12, 13] and [14], respectively) also gave estimations of the elastic constants c_{11} and c_{12} or at least their ratio but the accuracy of this approach seems to be rather limited. In particular, some values determined in such a manner (Ref. [14]) and suggested in Refs. [12, 13] differ even by a factor of three.

The aim of the present work was to apply some other independent techniques to determine the values of relevant elastic parameters as precisely as possible. The Brillouin light scattering, the Raman scattering, and *ab initio* calculations have been selected for this purpose.

2. Brillouin light scattering technique

In a BLS experiment, a beam of monochromatic light is used as a probe to reveal acoustic phonons that are naturally present in the medium under investigation. The power spectrum of these excitations is mapped out from frequency analysis of the light scattered within a solid angle, by means of a multipass Fabry–Perot interferometer. A number of acoustic modes confined within the film material can thus be revealed, and the elastic constants of the film determined [15–18].

The BLS experiments were performed at room temperature. The light source is an Ar^+ laser tuned on a 514.5 nm single mode line. Incident 100–500 mW p-polarized light is focused on the surface of the sample. The scattered light is analyzed by means of a Sandercock-type 3+3 pass tandem Fabry–Perot interferometer. For some spectra, an analyzer was inserted within the path of scattered light providing the s- or p- polarized part of the spectra. For the typical acquisition of a Brillouin spectrum from 2 to 4 hours was required. For a transparent layer a few microns thick, deposited on an opaque substrate, two different geometries of interaction contribute to the inelastic scattering of light from acoustic phonons in the layer [16, 17], as shown in the schematic wave vector diagram of Fig. 1. In

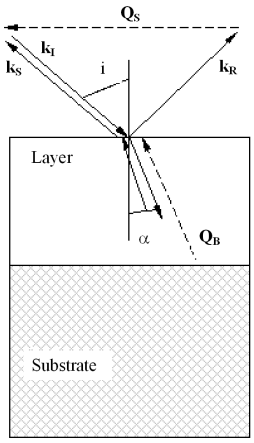

Fig. 1. Schematic diagram of interaction between photons and phonons (the backscattering geometry). Here $\boldsymbol{k}_{\mathrm{I}}$, $\boldsymbol{k}_{\mathrm{S}}$, and $\boldsymbol{k}_{\mathrm{R}}$ are the wave vector of incident, scattered, and reflected photons, respectively, while $\boldsymbol{Q}_{\mathrm{B}}$ and $\boldsymbol{Q}_{\mathrm{S}}$ are those of bulk and surface phonons, respectively.

the present work we used the backscattering geometry. In this condition the wave vector of the involved surface phonons propagating along the surface is determined by the relation

$$Q_{\mathrm{S}} = 2k_{\mathrm{I}} \sin(i), \tag{1}$$

where k_{I} denotes the optical wave vector in air and where i is the angle of inci-

dence. The wavelength of the surface phonons probed in this experiment is around 300 nm. The velocity (v_{S}) is deduced from the measured frequency (Ω) by the relation

$$v_{\mathrm{S}} = \Omega/Q_{\mathrm{S}}. \tag{2}$$

The wave vector of the involved bulk phonons is experimentally adjusted to the value

$$Q_{\mathrm{B}} = 2nk_{\mathrm{I}}, \tag{3}$$

where n is the refractive index of the film corresponding to the propagation direction of light inside the layer (isotropic for materials of cubic symmetry). The velocity (v_{B}) is deduced from the measured frequency (Ω) by the relation

$$v_{\mathrm{B}} = \Omega/Q_{\mathrm{B}}. \tag{4}$$

3. Samples preparation and structural characterizations

4 micrometer thick, zinc blende, MBE-grown monocrystalline MnTe layer and several short-period, CdTe/MnTe superlattices (SLs) were deposited on a (001) GaAs substrate covered by a 2 micrometer thick CdTe buffer layer. The growth of MnTe was realized in Te-rich conditions from elemental Mn and Te sources. Samples were grown in the Institute of Physics of the Polish Academy of Sciences in Warsaw (details of the growth were described elsewhere — see, e.g., [9, 19]). After the growth samples were characterized by the X-ray diffraction (XRD) in order to perform the crystal phase analysis, to determine the period of every SLs etc. In the case of thick MnTe layer the supplementary analysis with the use of the high-resolution, X-ray diffractometer in double crystal geometry and Cu K_{α_1} radiation was performed [19, 20]. XRD measurements were also performed for this sample with a four circles goniometer (INEL) using a cobalt anode. Epitaxial growth along the [001] direction (perpendicular to the substrate) was confirmed.

4. Results and discussion

The Brillouin spectra have been analyzed using a Green function approach of the equations of elasticity, with appropriate boundary conditions, in order to evaluate the spectral density of the displacements $u_z(z = 0)$, $u_y(z = 0)$, $u_x(z = 0)$ at the free surface [15], which are relevant for the frequency position of the lines observed in scattering from surface acoustic waves. The x-axis is along the propagation wave vector in the plane of the layer and the z-axis along the normal to this plane. The analysis of the surface waves for various directions of propagation from the [100] to the [110] axis enables us to measure the three independent elastic constants of ZB MnTe. In Fig. 2 we show spectra for two directions of propagation [100] and [110] axis in the (001) plane and an angle of

incidence $i = 60°$ with no polarization of the analyzed scattered electric field. The peaks labeled RW, PSM, SHM correspond, respectively, to the generalized Rayleigh surface wave, the pseudo-surface mode, and the shear horizontal mode, traveling parallel (or nearly parallel for the pseudo-surface modes) to the film surface. RW has a sagittal polarization only for the $\langle 100 \rangle$ high symmetry directions and SHM a quasi-shear horizontal polarization. PSM is a leaky wave that propagates nearly parallel to the surface and exists only for some planes of an anisotropic material over a finite range of propagation directions (in our case above $\phi \approx 27°$) and has a velocity higher than the bulk SHM mode. All these lines are reproduced in the relevant power spectrum of the displacement field components: u_x, u_y, and u_z calculated at the free surface (not shown in Fig. 2).

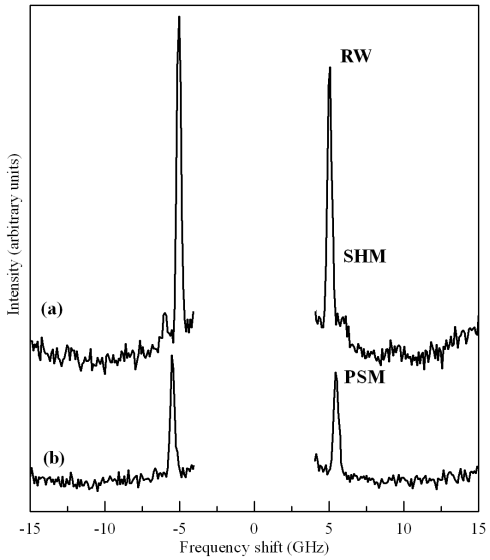

Fig. 2. Brillouin spectra obtained at room temperature from the epitaxial MnTe layer for the propagation of the surface acoustic waves along the [010] axis (a) and [110] axis (b). The angle of incidence is $i = 60°$, Ar^+ laser excitation line 514.5 nm. The peaks labeled RW, PSM, and SHM correspond, respectively, to the generalized Rayleigh surface wave, the pseudo-surface mode, and the shear horizontal mode, traveling parallel (or nearly parallel for the pseudo-surface modes) to the film surface.

The measurements of the frequency position of these Brillouin peaks provide the phase velocity v of the corresponding acoustic modes, according to Eq. (2). In addition to the analysis of the surface waves, we have also investigated the Brillouin spectra of the bulk waves that propagate almost normally to the surface of the layer. In general, the phase velocity of these waves depends also on c_{11} and c_{12} so the results of such measurements were used to check the previous data using the refractive index measured by the Raman scattering (see text below). The set

TABLE

Values of the three independent elastic constants of the ZB MnTe (c_{11}, c_{12}, c_{44}), the ratio $c_{11}/2c_{12}$, and the bulk modulus B given in the literature and determined in the present work. The Brillouin and Raman light scattering data made it possible to determine the refraction index value n for the Ar^+ laser excitation line. Due to the fact that n influences the elastic constant value c_{11} (determined by the Raman scattering) and for a given c_{11} value c_{12} (both determined by the Brillouin scattering) we used for BLS the same refraction index value resulting from the Raman scattering analysis.

	c_{11} [GPa]	c_{44} [GPa]	c_{12} [GPa]	$c_{11}/2c_{12}$	Bulk modulus [GPa] $(c_{11}+2c_{12})/3$
This work:					
Brillouin, $n = 2.85$	50 ± 1	14.7 ± 0.3	31 ± 1	0.806	37
Raman, $n = 2.85$	52 ± 4	–	–	–	–
Theory, GGA (LSDA)	–	–	–	–	29 (50)
J. Appl. Phys. **81**, 6120 (1997)	–	–	–	0.77 ± 0.15	–
Phys. Rev. B **49**, 4619 (1994)	22.2 ± 1	–	11.6 ± 1	0.956	–
Phys. Rev. B **31**, 5212 (1985) (bulk $Cd_{0.48}Mn_{0.52}Te$)	51.0 ± 1	18.5 ± 0.2	35 ± 1	0.72	–
Appl. Phys. Lett. **64**, 49 (1994)	≈ 60	–	≈ 49	0.61	–

of obtained elastic parameters of the ZB MnTe is listed in Table together with the literature data. Directly determined values of the elastic constants are close to these corresponding to bulk $Cd_{1-x}Mn_xTe$ mixed crystal.

In order to check selected values determined by the Brillouin scattering, the Raman scattering measurements were also performed at room temperature in the quasi-backscattering geometry on CdTe/MnTe SLs. 514.5 nm Ar^+ laser line was used for the excitation. Raman scattering was applied in order to observe folded acoustic phonon modes for CdTe/MnTe SL (Fig. 3). Using various superlattices of different periods for which the two components of the $m = 1$ doublet are observable, the elastic coefficient c_{11} of MnTe could be determined by a simple fit (the details of the Raman scattering measurements will be described elsewhere). The found values of c_{11} (52.0 ± 4 GPa) is in excellent agreement with the results given by the Brillouin experiments. From the values of the splitting between the two

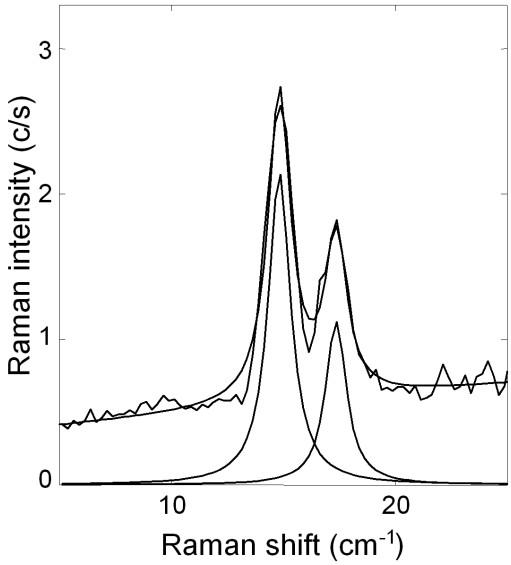

Fig. 3. An example of the Raman scattering spectrum obtained at room temperature on $(CdTe)_{12}/(MnTe)_8$ superlattice. The structures seen in this figure correspond to the well split doublet of the first-order folded acoustic phonons. Smooth curves represent the results of a fit allowing to extract the frequencies of both components of the doublet.

components of the doublet and knowing the value of the refraction index of CdTe ($n = 3.15$ [21]) it was also possible to determine a value of the refraction index of MnTe ($n = 2.85 \pm 0.15$) in fair agreement with the value $n = 2.974$ computed through a Kramers–Kronig analysis of a reflectivity spectrum, taken some time ago on bulk MnTe [22].

Structural properties of ZB MnTe were determined by *ab initio* calculations making use of the density functional theory and atomic pseudopotentials. Both the local spin density approximation (LSDA) and the generalized gradient approximation (GGA) were used in the calculations. The spin polarization of the antiferromagnetic (AF) MnTe was taken into account, but in order to simplify the calculations a less complicated magnetic structure AF type-I was assumed instead of the actual type-III. We have checked that this particular choice of the magnetic ordering has no significant influence on the numerical results: the calculated energy difference between type-I and type-III orderings for the equilibrium value of the lattice parameter is 0.002 eV per atom only. The energy of the ferromagnetic ordering is 0.075 eV per atom higher. The calculated lattice parameter using LSDA (GGA) is 6.100 (6.303) Å, i.e., the GGA gives a better agreement with the experimental value 6.338 Å. Similarly, the bulk modulus calculated within the GGA, $B = 29$ GPa, is closer to the experimental value determined in this work (37 GPa, see Table) than that obtained within LSDA, 50 GPa.

5. Summary and conclusion

We have determined, using the Brillouin light scattering, the elastic properties of zinc blende, MBE-grown MnTe layer. Values of three independent elastic constants c_{11}, c_{12}, and c_{44} have been successfully measured for this phase of investigated compound. The c_{11} was derived from the bulk longitudinal wave propagating nearly normal to the film plane while c_{44} was obtained from the shear horizontal wave that propagates parallel to the film plane. The c_{12} constant was derived from the Rayleigh surface mode and the pseudo-surface mode. The obtained value of c_{11} is in a very good agreement with that resulting from the Raman scattering results from CdTe/MnTe superlattices. The values of the lattice constant and bulk modulus obtained from *ab initio* GGA calculations are in reasonable agreement with the experiment.

Acknowledgments

We would like to express our gratitude to Prof. J. Dobaczewski for his kind help in some numerical calculations. This work was supported in part within European Community programs ICA1-CT-2000-70018 (Centre of Excellence CELDIS) and G1MA-CT-2002-4017 (Centre of Excellence CEPHEUS), by the grant PBZ/KBN/044/P03/2001 from the State Committee for Scientific Research (Poland), and by ACI NR0095 "NANODYNE" from the French Ministry of National Education and Research.

References

[1] F. Nizzoli, J.R. Sandercock, in: *Dynamical Properties of Solids*, Eds. G.K. Horton, A.A. Maradudin, Vol. 6, North-Holland, Amsterdam 1990, p. 281.

[2] C. Thomsen, H.T. Grahn, H.J. Maris, J. Tauc, *Phys. Rev. B* **34**, 4129 (1986).

[3] G.E. Heinen, J.E. Hilliard, *J. Appl. Phys.* **54**, 728 (1983).

[4] C.M. Su, M. Wuttig, *J. Alloys Comp.* **211/212**, 428 (1994).

[5] J. Woirgard, J.C. Dargenton, *Meas. Sci. Technol.* **6**, 16 (1995).

[6] P. Goudeau, P.O. Renault, P. Villain, C. Coupeau, V. Pelosin, B. Boubeker, K.F. Badawi, D. Thiaudière, M. Gailhanou, *Thin Solid Films* **398-399**, 496 (2001).

[7] W. Sharpe, Jr., *Mater. Res. Soc. Symp. Proc.* **444**, 185 (1996).

[8] B. Yuan, W. Sharpe, Jr., *Experimental Techniques* **21**, 32 (1997).

[9] E. Janik, E. Dynowska, J. Bak-Misiuk, M. Leszczyński, W. Szuszkiewicz, T. Wojtowicz, G. Karczewski, A.K. Zakrzewski, J. Kossut, *Thin Solid Films* **267**, 74 (1995).

[10] T.M. Giebultowicz, P. Kłosowski, N. Samarth, H. Luo, J.K. Furdyna, J.J. Rhyne, *Phys. Rev. B* **48**, 12817 (1993).

[11] P. Maheswaranathan, R.J. Sladek, U. Debska, *Phys. Rev. B* **31**, 5212 (1985).

[12] J.R. Buscheret, F.C. Peiris, N. Samarth, H. Luo, J.K. Furdyna, *Phys. Rev. B* **49**, 4619 (1994).

[13] E. Abramof, W. Faschinger, H. Sitter, A. Pesek, *Appl. Phys. Lett.* **64**, 49 (1994).

[14] M. de Naurois, J. Stangl, W. Faschinmger, G. Bauer, S. Ferriera, *J. Appl. Phys.* **81**, 6120 (1997).

[15] P. Djemia, Ph.D. thesis, Université Paris Nord, 1998.

[16] P. Djemia, Y. Roussigné, G.F. Dirras, K.M. Jackson, *J. Appl. Phys.* **95**, 2324 (2004).

[17] P. Djemia, C. Dugautier, T. Chauveau, M.I. De Barros, L. Vandenbulcke, *J. Appl. Phys.* **90**, 3771 (2001).

[18] P. Moch, P. Djemia, F. Ganot, *Vide* **301**, 3771 (2001).

[19] W. Szuszkiewicz, E. Dynowska, J. Bak-Misiuk, G. Karczewski, T. Wojtowicz, J. Kossut, *Acta Phys. Pol. A* **90**, 1090 (1996).

[20] B. Hennion, W. Szuszkiewicz, E. Dynowska, E. Janik, T. Wojtowicz, *Phys. Rev. B* **66**, 224426 (2002).

[21] S. Adashi, T. Kimura, N. Suzuki, *J. Appl. Phys.* **74**, 3435 (1993).

[22] B.J. Kowalski, E. Guziewicz, B.A. Orłowski, E. Janik, G. Karczewski, T. Wojtowicz, J. Kossut, T. van Gemmeren, T. Buslaps, R.L. Johnson, *Thin Solid Films* **267**, 69 (1995).